Photoelectron spectra of the $C_{2n}H^-$ ($n=1-4$) and $C_{2n}D^-$ ($n=1-3$) anions

Travis R. Taylor, Cangshan Xu,[a] and Daniel M. Neumark
Department of Chemistry, University of California, Berkeley, California 94720 and Chemical Sciences Division, Lawrence Berkeley National Laboratory, Berkeley, California 94720

(Received 12 January 1998; accepted 19 March 1998)

Anion photoelectron spectra of the carbon monohydrides, $C_{2n}H^-$ for $n=1-4$ and $C_{2n}D^-$ for $n=1-3$, have been measured. The spectra were recorded at a wavelength of 266 nm (4.657 eV) and yield electron affinities for each species. The spectra are vibrationally resolved, and some of the vibrational modes in the neutral $C_{2n}H(D)$ radicals are assigned. In addition, photoelectron angular distributions allow one to distinguish between photodetachment transitions to the $^2\Sigma^+$ and $^2\Pi$ states of the neutrals. The spectra confirm previous work showing that C_2H and C_4H have $^2\Sigma^+$ ground states, while C_6H and C_8H have $^2\Pi$ ground states. In addition, we observe the low-lying $^2\Pi$ or $^2\Sigma^+$ excited states for all four radicals. The photoelectron angular distributions also serve as a probe of vibronic coupling between the $^2\Sigma^+$ and $^2\Pi$ states. These effects are particularly prominent in the C_2H^- and C_4H^- spectra. © *1998 American Institute of Physics.* [S0021-9606(98)01724-3]

I. INTRODUCTION

Bare carbon clusters, C_n, have been extensively studied over the past decade using experiment[1–18] and theory.[19–29] The related carbon monohydrides, C_nH, which play an important role in combustion[30] and interstellar chemistry, have received somewhat less attention. Several C_nH chains[31–36] have been observed in the interstellar medium. In addition, C_nH radicals are candidates for the diffuse interstellar bands.[37] Through microwave spectroscopy the ground vibrational and electronic states have been well characterized and several of these species have been identified in the interstellar medium.[38–40] However, the vibrational and electronic spectroscopy of these open shell species is complicated by the presence of close-lying $^2\Sigma$ and $^2\Pi$ electronic states. For example, the $\tilde{X}\ ^2\Sigma^+$ state ground state of C_2H interacts strongly with the nearby $\tilde{A}\ ^2\Pi$ state. In C_4H, the $^2\Sigma$ and $^2\Pi$ states are nearly degenerate. In C_6H and C_8H the $^2\Pi$ state is the ground state; a low-lying $^2\Sigma$ state is expected in each case but its term value is unknown. In this paper we use negative ion photoelectron spectroscopy of the carbon monohydride anions $C_{2n}H^-$ ($n=1-4$) and $C_{2n}D^-$ ($n=1-3$) as a means of probing the electronic and vibrational spectroscopy of the neutral species. Our experiments provide new insight concerning the energetics and interactions of the $^2\Sigma$ and $^2\Pi$ states, and represent the first measurements of the electron affinities for C_4H, C_6H, and C_8H.

The ethynyl radical, C_2H, is the most thoroughly studied of the C_nH species. Experimental techniques applied to this radical include electron spin resonance (ESR),[41–43] laser magnetic resonance,[44,45] microwave and millimeter-wave spectroscopy,[46–49] matrix isolation infrared spectroscopy,[50–54] color center and diode laser spectroscopy,[55–64] Fourier transform infrared (FTIR) emission spectroscopy,[65] laser-induced fluorescence (LIF),[65–67] and photoelectron spectroscopy of the C_2H^- anion.[68] Extensive theoretical work on the spectroscopy of C_2H has also been carried out.[69–71] These investigations have focused primarily on the infrared region, which probes the vibrational transitions within the $\tilde{X}\ ^2\Sigma^+$ state as well as electronic transitions to the low-lying $\tilde{A}\ ^2\Pi$ state, for which $T_0 \approx 3600-3700$ cm^{-1}. Further information comes from photodissociation experiments[72–77] on C_2H_2 in which the $H+C_2H$ translational energy distribution reveals vibrational progressions in both states of C_2H. Even though several of these spectra are of sufficient resolution to fully resolve rotational and fine structure, assignment of the observed bands has been far from straightforward due to strong vibronic coupling between the $\tilde{X}\ ^2\Sigma^+$ and $\tilde{A}\ ^2\Pi$ states as well as Fermi resonance interactions within the $\tilde{X}\ ^2\Sigma^+$ state. Thus, for example, no single band corresponding to the $\tilde{A}$-$\tilde{X}$ vibrational origin has been observed, because the $\tilde{A}(000)$ vibrational ground state is strongly coupled to several nearby vibrationally excited levels of the $\tilde{X}$ state.

In the first spectroscopic observation of C_4H, its optical, infrared, and ESR spectra were obtained via matrix isolation spectroscopy.[78] It was later identified in the interstellar medium through its millimeter-wave spectrum.[31] Subsequently, several laboratory microwave spectroscopy studies have been performed,[38,79–81] and an FTIR study in a rare gas matrix[82] yielded a more complete set of vibrational frequencies for the ground state. Several *ab initio* studies have been carried out on C_4H in which geometries, vibrational frequencies, and electronic term values were calculated.[30,81,83–87] The experiments indicate that C_4H has a $^2\Sigma^+$ ground state, but the *ab initio* calculations indicate that the lowest $^2\Sigma^+$ and $^2\Pi$ states are nearly degenerate. Most of the calculations[81,85,86] agree with the experimental assignment of the $^2\Sigma$ state as the ground state but place the $^2\Pi$ state within 100 cm^{-1}, although two calculations[84,87] predict the $^2\Pi$ state to be the ground state. As previously mentioned the $\tilde{X}\ ^2\Sigma^+$ and $\tilde{A}\ ^2\Pi$ states are nearly degenerate, increasing the oppor-

[a]Current address: Lam Research Corporation, 9713 Bayside Parkway, Fremont, CA 94538.

tunity for vibronic coupling between the two electronic states. Perturbed rotation lines in the millimeter wave spectra[33,79] provide evidence of the vibronic interaction. Recent LIF results[88] on the $\tilde{B}\ ^2\Pi \leftarrow \tilde{X}\ ^2\Sigma^+$ transition can only be explained by invoking vibronic coupling between the $\tilde{X}\ ^2\Sigma^+$ and $\tilde{A}\ ^2\Pi$ states. In this work we directly observe the $\tilde{A}\ ^2\Pi$ state and the effects of its coupling with the ground state.

A millimeter-wave spectrum assigned to the C_6H radical was first observed in the envelope of a carbon star;[32] this assignment was subsequently confirmed in laboratory measurements.[39] Both studies indicated that C_6H has a $^2\Pi$ ground state. The only other laboratory measurements have been in cryogenic matrices by Graham and co-workers[89] using FTIR spectroscopy and by Maier and co-workers[13,15] using electronic absorption. Several *ab initio* studies have also been carried out in which geometries, vibrational frequencies, term values, and various thermodynamic quantities were calculated.[30,83–85,87,90–93] The calculations predict a low-lying $^2\Sigma^+$ state which has not been observed experimentally.

The C_8H radical is the least studied of the species considered here. As with C_6H, it was also first seen in the envelope of a carbon star[36] with its assignment confirmed by laboratory measurements.[40] An electronic absorption band in the visible region was seen by Maier and co-workers.[15] Electronic excitation energies have been calculated.[83,87]

Here we report vibrationally resolved photoelectron spectra of $C_{2n}H^-$ $(n=1-4)$ and $C_{2n}D^-$ $(n=1-3)$. The anions are closed-shell $^1\Sigma$ species, and in all cases the lowest $^2\Sigma$ and $^2\Pi$ neutral states are accessible by anion photodetachment. We also obtain photoelectron angular distributions which can be used to distinguish between transitions to the two neutral states. This is particularly useful in analyzing the C_2H^- and C_4H^- spectra in which the two bands are strongly overlapped.

II. EXPERIMENT

The anion photoelectron spectrometer used in this study has been described in detail previously.[94,95] In the work presented here, a mixture of 4% C_2H_2 and 1% CO_2 in a balance of Ne is expanded through a pulsed piezoelectric valve at a backing pressure of 40 psi. The resulting molecular beam passes through a pulsed electric discharge assembly,[96] and C_nH^- anions are formed by firing the discharge during the molecular beam pulse. The negative ions pass through a skimmer into a differentially pumped region. They are extracted perpendicular to their flow direction by a pulsed electric field and injected into a linear reflectron time-of-flight (TOF) mass spectrometer,[97,98] affording a mass resolution $m/\Delta m$ of 2000. The ions of interest are selectively photodetached with the fourth harmonic of a pulsed Nd:YAG laser (266 nm, $h\nu=4.657$ eV). The electron kinetic energy (eKE) distribution is determined by TOF analysis. The energy resolution is 8 meV at 0.65 eKE and degrades as $(\mathrm{eKE})^{3/2}$ at higher eKE. The laser polarization can be rotated by means of a half wave plate, and each photoelectron spectrum is measured at at least two polarization angles θ, defined with respect to the electron detection axis, in order to characterize the photoelectron angular distribution. Secondary electrons initiated by scattered photons necessitate the collection and subtraction of background spectra.

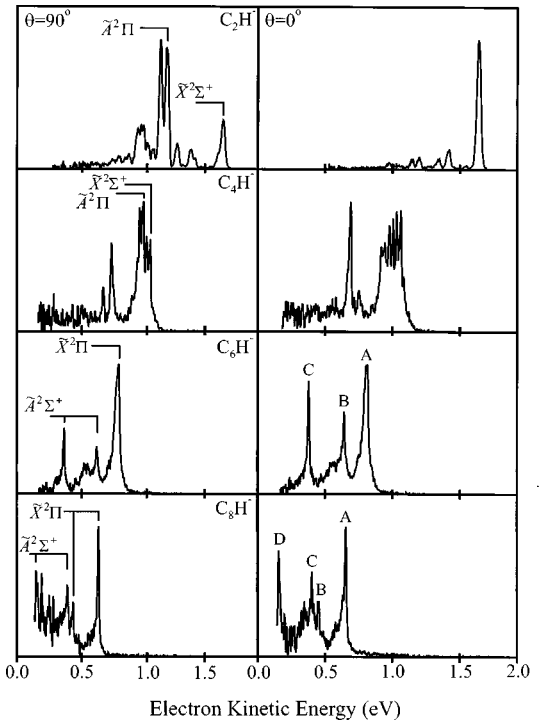

FIG. 1. Photoelectron spectra of $C_{2n}H^-$ for $n=1-4$ taken at the photodetachment wavelength of 266 nm (4.657 eV). Laser polarization angles are $\theta=0°$ and 90° with respect to the direction of electron collection.

III. RESULTS

Figure 1 shows the photoelectron spectra of the carbon monohydride anions $C_{2n}H^-$ $(n=1-4)$ taken at the polarization angles of $\theta=0°$ and 90° with a photon energy of 4.67 eV. The photoelectron spectra of $C_2H(D)^-$ and $C_4H(D)^-$ are presented in more detail in Figs. 2 and 3, respectively.

In these and all other photoelectron spectra the electron kinetic energy, eKE, is related to the internal energy of the neutral and anion by

$$\mathrm{eKE}=h\nu-EA-E^0+E^-. \tag{1}$$

Here, $h\nu$ is the photon energy, EA is the adiabatic electron affinity, E^0 is the internal energy of the neutral, and E^- is the internal energy of the anion. Rotational energy contributions are neglected. As indicated by Eq. (1) the peaks occurring at lowest eKE in the photoelectron spectrum correspond to the highest internal energy states of the neutral.

The photoelectron differential cross section[99] is given as

$$\frac{d\sigma}{d\Omega}=\frac{\sigma_{\mathrm{total}}}{4\pi}\left[1+\frac{\beta(E)}{2}\,(3\cos^2\,\theta-1)\right]. \tag{2}$$

The polarization angle, θ, is the angle between the electric vector of the photon and the axis along which the electrons are detected. The differential cross section is parametrized in

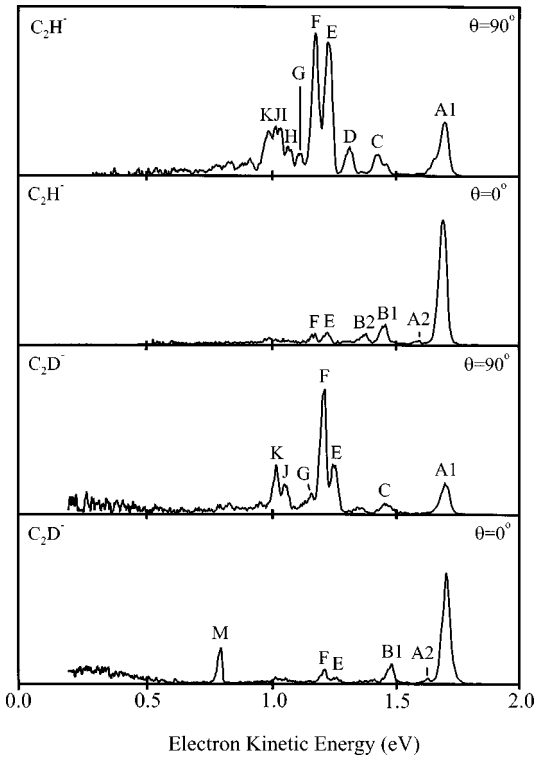

FIG. 2. Photoelectron spectra of $C_2H(D)^-$ taken at the photodetachment wavelength of 266 nm (4.657 eV). Laser polarization angles are $\theta=0°$ and 90° with respect to the direction of electron collection.

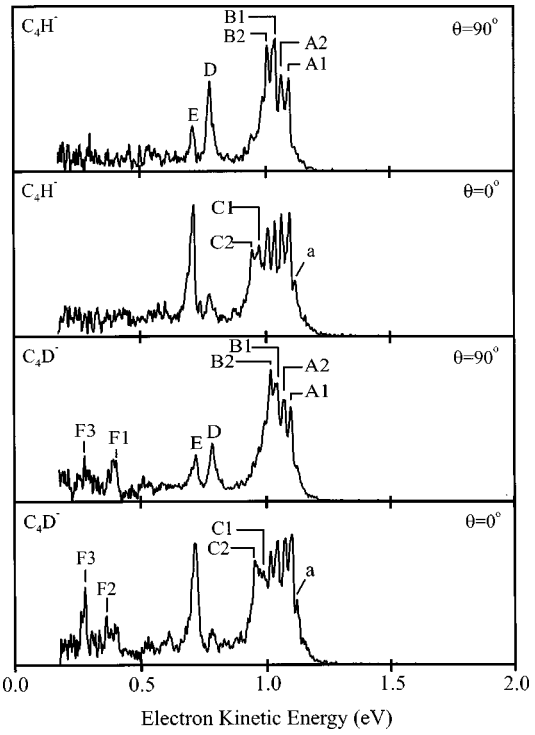

FIG. 3. Photoelectron spectra of $C_4H(D)^-$ taken at the photodetachment wavelength of 266 nm (4.657 eV). Laser polarization angles are $\theta=0°$ and 90° with respect to the direction of electron collection.

terms of the anisotropy parameter, β, for which $-1\leqslant\beta\leqslant 2$. The anisotropy parameter for a particular peak is obtained from the relative peak intensities taken at different polarization angles. Peaks with differing values of β generally result from transitions to different neutral electronic states, so this is a useful means of assigning electronic states and distinguishing contributions from overlapping electronic bands. Values of β for all spectra are listed in Tables I–IV.

As n increases for the $C_{2n}H$ species the spectral features shift to lower eKE, indicating an increase in electron affinity. The relative intensities of the peaks in the $\theta=90°$ and $\theta=0°$ spectra of all anions change dramatically, indicating the presence of transitions to at least two electronic states.

Figure 2 shows the photoelectron spectra of $C_2H(D)^-$ at 4.657 eV taken at laser polarization angles $\theta=90°$ and $\theta=0°$. Peaks $A1-C$ were observed at higher resolution in the photoelectron spectrum taken by Ervin *et al.*[68] at 3.531 eV, but the higher photon energy used in our experiment yields many more peaks. The spectra in Fig. 2 show resolved vibrational structure. Peaks $A1-B2$ at high eKE have strongly positive β parameters, while $\beta<0$ for peaks $C-K$. This generally indicates the presence of transitions to two electronic states of the neutral, a result expected for C_2H with its close-lying $^2\Sigma^+$ and $^2\Pi$ states. The energy shifts upon isotopic substitution are sufficiently small so that one can easily correlate peaks in the C_2D^- and C_2H^- spectra. The intensity distribution of the peaks in the C_2D^- spectra differs substantially from the C_2H^- spectra. Peak F is considerably larger in the C_2D^- spectra and the relative intensities of peaks C, D, E, $G1$, and J are significantly lower. On the other hand, peak M appears in the C_2D^- $\theta=0°$ spectrum but not in the C_2H^- spectra.

The C_4H^- and C_4D^- spectra in Figs. 1 and 3 consist of a partially resolved group of at least six peaks around eKE=1.0 eV (peaks $A1-C2$), and two more isolated features, peaks D and E, at lower eKE. The C_4H^- and C_4D^- are similar, except for some small peaks below 0.5 eV that appear only in the C_4D^- spectrum. As with $C_2H(D)^-$, the relative peak intensities vary strongly with laser polarization, particularly in the group of peaks around 1.0 eV, indicating the presence of at least two overlapping electronic states. The spectral features in Fig. 3 can be classified into three groups according to their β parameter and energy. Peaks $A1-A2$, $C1-C3$, and E have $\beta>0$ and are most prominent at $\theta=0°$. Peaks $B1-B2$ and D have $\beta\leqslant 0$ and peaks $F1-F3$ have $\beta>0$ and lie at a much higher energy than the first group.

The C_6H^- and C_8H^- spectra each show several distinct peaks superimposed on broad underlying signal. The peak positions and anisotropy parameters are listed in Table IV. The photoelectron angular distributions indicate that transitions to two electronic states contribute to each spectrum. In the C_6H^- spectra, peak A decreases in intensity relative to peaks B and C as the laser polarization is rotated from 90° to 0°. In the C_8H^- spectra, a similar trend is seen for peaks A and B relative to peaks C and D.

IV. ANALYSIS AND DISCUSSION

A. General considerations

The analyses for most photoelectron spectra are valid within the Franck–Condon (FC) approximation, which relies

on the assumption that the electronic and vibrational wave functions are separable. The transition intensity, I, is governed by

$$I \propto |\tau_e|^2 |\langle \psi^-_{\nu''} | \psi^0_{\nu'} \rangle|^2. \quad (3)$$

Here τ_e is the electronic transition dipole moment and $|\langle \psi^-_{\nu''} | \psi^0_{\nu'} \rangle|^2$ is the Franck–Condon factor for the vibrational wave functions of the negative ion and corresponding neutral. If the anion and neutral are linear, one therefore expects vibrational progressions in the totally symmetric stretching modes. Transitions involving even changes of bending quanta can also be observed if there is a sufficiently large change in the vibrational frequency of a bending mode upon photodetachment. The photoelectron spectra of linear C_n^- clusters are explained within the FC approximation as discussed by Arnold *et al.*[3]

However, the previous photoelectron spectrum[68] of C_2H^- showed activity in the C_2H bending mode (ν_2), including transitions in which $\Delta\nu$ is odd, even though the anion and neutral are linear. In addition, many transitions in the infrared spectra of C_2H which are nominally between two vibrational levels of the $\tilde{X}\ ^2\Sigma^+$ state show a significant spin-orbit splitting in the upper state.[100] Both observations are attributed to strong vibronic coupling effects because of the close-lying $\tilde{X}\ ^2\Sigma^+$ and $\tilde{A}\ ^2\Pi$ states in C_2H, resulting in nonseparability of the electronic and vibrational wave functions. The nature of the vibronic coupling in C_2H, a combination of Renner–Teller coupling within the $\tilde{A}\ ^2\Pi$ state and Herzberg–Teller coupling between the $\tilde{X}\ ^2\Sigma^+$ and $\tilde{A}\ ^2\Pi$ states, has been explored in a series of theoretical papers by Peric *et al.*[69–71] It is unusually strong in C_2H because of a low-energy intersection between the $^2\Sigma^+$ and $^2\Pi$ states for linear geometries.

Although the resolution of anion photoelectron spectroscopy is not nearly as high as many of the other techniques used to investigate C_2H, the photoelectron angular distributions provide insight into the vibronic coupling between the $\tilde{X}\ ^2\Sigma^+$ and $\tilde{A}\ ^2\Pi$ states that is generally not available elsewhere. This connection was demonstrated in the original photoelectron spectrum[68] and is further amplified in the spectra presented here at higher photon energy. Since the larger $C_{2n}H$ radicals studied here also have close-lying $^2\Sigma^+$ and $^2\Pi$ states, one expects vibronic coupling to play a role in the photoelectron spectra of the corresponding $C_{2n}H^-$ anions. An understanding of vibronic coupling in the C_2H^- spectra can therefore be used to interpret similar effects in the spectra of the larger anions.

B. $C_2H(D)$

The C_2H^- anion is linear with a $(\ldots 4\sigma^2 1\pi^4 5\sigma^2)\ ^1\Sigma^+$ ground state. One-electron detachment from the ground state anion can produce the ground $\tilde{X}\ ^2\Sigma^+$ $(\ldots 4\sigma^2 1\pi^4 5\sigma^1)$ and first excited $\tilde{A}\ ^2\Pi$ $(\ldots 4\sigma^2 1\pi^3 5\sigma^2)$ neutral states, so transitions to both states of C_2H should be observable in the photoelectron spectra. In the absence of vibronic coupling, one therefore would expect to see two sets of peaks, possibly with differing β values, that correspond to transitions to vibrational levels of the two electronic states. The discussion below shows that the situation is considerably more complex.

As a result of the considerable spectroscopic work already carried out on C_2H and C_2D, many of the peaks seen in the photoelectron spectrum can be correlated with previously observed and assigned peaks. These correspondences are shown in Tables I and II. The two most prominent peaks are $A1$ and F, which correspond to transitions to the (000) level of the $\tilde{X}\ ^2\Sigma^+$ state and the (01^-0) level of the $\tilde{A}\ ^2\Pi$ state, respectively. The two peaks have very different angular distributions, with $\beta \cong 1$ for peak $A1$ and $\beta \cong -1$ for peak F. The $\tilde{A}(01^-0)$ level has Σ^- vibronic symmetry ($K=0$) but pure Π electronic character; it is not vibronically coupled to the $\tilde{X}\ ^2\Sigma^+$ state.[42] We can therefore associate positive values of β with peaks that have largely Σ electronic character and negative values of β with transitions to states with significant Π character, or which are allowed only because of vibronic coupling to the $\tilde{A}\ ^2\Pi$ state.

Peaks $A1$, $A2$, $B1$, and $B2$ are the only peaks in the C_2H^- spectrum with $\beta > 0$. This is consistent with the assignments in Table I, which show them all to be fully allowed transitions to $\tilde{X}$ state vibrational levels. On the other hand, peaks C and D are each assigned as a pair of overlapped transitions to the $\tilde{X}(011)/\tilde{X}(050)$ and $\tilde{X}(031)/\tilde{X}(070)$ levels, respectively. These transitions are only allowed through vibronic coupling to an $\tilde{A}$ state level with the same (Π) vibronic symmetry, and this is consistent with the negative β values observed for these peaks.

Next to peak F, peak E is the most intense of the peaks with $\beta < 0$. It lies 3750 cm^{-1} from peak $A1$, which is in the vicinity of the estimated origin of 3772 cm^{-1} for the $\tilde{A}-\tilde{X}$ transition.[60] Comparison with high resolution data indicates that Peak E is composed of several features; three previously observed vibrational bands at 3600, 3692, and 3786 cm^{-1} all lie within the envelope of peak E (275 cm^{-1}).[56,58,63,100] The observation of multiple bands results from strong mixing of the $\tilde{A}(000)$ level with nearby $\tilde{X}$ state levels of the appropriate symmetry.

Similar effects are seen in this energy range in the C_2D^- spectra. Peaks $A1$, $A2$, and $B2$ have positive values of β, as expected from their assignments, whereas $\beta < 0$ for peaks C and E. Peak C is assigned to the $\tilde{X}(011)$ transition, and is therefore allowed only by vibronic coupling. Just as in the C_2H^- spectra, peak E at 3594 cm^{-1} lies in the range of the estimated $\tilde{A}$ state origin, 3697 cm^{-1}.[60] Stephens *et al.*[60] observed a band in C_2D at 3513 cm^{-1}. Although Peric[101] assigns this band to the $\tilde{A}(000)$ origin, it is clear that $\tilde{X}$ state levels are mixed in because the spin-orbit coupling constant in the upper state (-6.3 cm^{-1}) is considerably less than it would be for a pure $\tilde{A}$ state (~ -25 cm^{-1}). In any case, the 100 cm^{-1} offset of peak E relative to the 3513 cm^{-1} band suggests that it results from an overlapped transition. It is not clear what this might be because no transitions between 3600 and 3700 cm^{-1} [originating from the $\tilde{X}(000)$ level] have been seen in either gas phase or matrix absorption[53] experiments.

TABLE I. Peak positions and spectral assignments for the C_2H^- photoelectron spectra.

Peak	Assignment	Position (eV)	Splitting from peak $A1$ (cm^{-1})[a]	β[b]	Previous observations[c]	Ref.
$A1$	$\tilde{X}$ (000)	1.699	0	1.04	0	
$A2$	$\tilde{X}$ (020)	1.602	783	0.98	760	k
$B1$	$\tilde{X}$ (001)	1.468	1866	0.87	1841	h
C	$\tilde{X}$ (011), $\tilde{X}$ (050)	1.435	2136	−0.58	2091, 2166	i,k
$B2$	$\tilde{X}$ (021)	1.389	2505	1.29	2550	l
D	$\tilde{X}$ (031), $\tilde{X}$ (070)	1.319	3064	−0.99	2928, 3101	n,k
E	$\tilde{X}$ (051), $\tilde{A}$ (00^00)	1.236	3740	−0.95	3786, 3686[d]	k,f
F	$\tilde{A}$ (01^-0)	1.184	4155	−0.96	4143	f
G	$\tilde{X}$ (071), $\tilde{A}$ (02^-0)	1.123	4651	−0.73	4697	o
H	$\tilde{X}$ (0110)	1.077	5017	−0.76	5005, 4987	o
I	$\tilde{A}$ (01^+0)	1.044	5287	−1.02	5083[d]	e
J	$\tilde{X}$ (0120)	1.024	5445	−0.91	5403	m,j,g
K	$\tilde{A}$ (091)	0.999	5649	−0.88	5602[d]	e

[a]Error ± 50 cm^{-1}
[b]Average error ±0.25.
[c]All values rounded to the nearest whole number.
[d]Neon matrix value as noted, all other values are gas phase.
[e]Reference 53.
[f]Reference 56.
[g]Reference 60.
[h]Reference 61.
[i]Reference 63.
[j]Reference 65.
[k]Reference 67.
[l]Reference 68.
[m]Reference 76.
[n]Reference 100.
[o]Reference 103.

For both isotopes, $\beta<0$ for all peaks with lower electron energy than peak F (except peak M in C_2D^-). As shown in Tables I and II, many of these peaks correspond to transitions that have been seen previously in either gas phase or matrix experiments and assigned to particular $\tilde{X}$ or $\tilde{A}$ state transitions. Implicit in these assignments is the notion that virtually all of these states are vibronically coupled to various $\tilde{A}$ state levels; this is supported by the theoretical work of Peric *et al.*[70,71,101] Our photoelectron angular distributions explicitly show that all of the transitions in this energy region correspond to neutral states with significant $\tilde{A}$ state character, and that this mixing with the $\tilde{A}$ state accounts for essentially all of the intensity in the photoelectron spectrum. Given the overlapped appearance of many of the peaks in this energy range, it is difficult to make more definitive assignments than those already listed in Tables I and II.

TABLE II. Peak positions and spectral assignments for the C_2D^- photoelectron spectra.

Peak	Assignment	Position	Splitting from peak $A1$ (cm^{-1})[a]	β[b]	Gas phase[c]	Ref.
$A1$	$\tilde{X}$ (000)	1.701	0	1.51		
$A2$	$\tilde{X}$ (020)	1.627	598	1.45	605	h
$B1$	$\tilde{X}$ (001)	1.481	1774	1.37	1743	g
C	$\tilde{X}$ (011)	1.463	1920	0.28	2015	h
E	$\tilde{A}$ (00^00)	1.256	3594	−0.46	3513	f
F	$\tilde{A}$ (01^-0)	1.213	3940	−0.58	3999	f
G	$\tilde{A}$ (02^-0)	1.162	4345	−0.56	4384[d]	e
J		1.059	5179	−0.3	5206	f
K		1.023	5469	−0.54	5460	f
M		0.797	7295	1.59		

[a]Error ±50 cm^{-1}.
[b]Average error ±0.25.
[c]All values are rounded to the nearest whole number.
[d]Neon matrix value as noted, all other values are gas phase.
[e]Reference 53.
[f]Reference 60.
[g]Reference 62.
[h]Reference 68.

C. $C_4H(D)$

The C_4H^- and C_4D^- spectra each exhibit a partially resolved group of at least six peaks, $A1-C2$ around eKE=1.0 eV. Peaks $A1-B2$ are approximately evenly spaced with an average spacing of 223 cm^{-1}, and peaks $C1$ and $C2$ are separated by 226 cm^{-1}. This spacing is close to calculated frequencies by Kiefer *et al.*[30] for the ν_7 bend mode in the $^2\Sigma^+$ and $^2\Pi$ states of C_4H. All other calculated frequencies are considerably higher. Thus, independently of the detailed peak assignments, it is clear that we observe strong $\Delta v=1$ transitions in a nontotally symmetric bending mode even though the anion and relevant neutral states are linear. As in the C_2H^- photoelectron spectra, this is a signature of a breakdown in the Franck-Condon approximation caused by vibronic coupling between nearby Σ and Π electronic states.

C_4H^- is a $^1\Sigma^+$ species with molecular orbital configuration $\ldots 1\pi^4 2\pi^4 9\sigma^2$. The lowest neutral $^2\Sigma^+$ and $^2\Pi$ states are formed by photodetachment from the 9σ and 2π orbitals, respectively. As mentioned in the Introduction, these states are believed to be nearly degenerate, with the $^2\Sigma^+$ state lying slightly lower in energy, so one might expect transitions to these electronic states to overlap in the photoelectron spectrum. In our spectra, the anisotropy parameters for peaks $A1-C2$ imply that this group of peaks indeed consists of overlapped electronic transitions; we find $\beta>0$ for peaks $A1$, $A2$, $C1$, and $C2$, whereas $\beta\cong 0$ for peaks $B1$ and $B2$. By analogy with the C_2H^- photoelectron angular distributions, we assign the peaks with $\beta>0$ to transitions to the $^2\Sigma^+$ state, and peaks $B1$ and $B2$ to transitions to the $^2\Pi$ state. Given that this group of peaks most likely consists of overlapped vibrational progressions in the two electronic states, these assignments represent the dominant rather than the sole electronic character of the neutral level.

We now consider the peak assignments in more detail. The assignment of peaks $A1$ and $A2$ to the $^2\Sigma^+$ state implies that this is the ground electronic state of C_4H, a result consistent with previous experiments and most calculations. Peak $A1$ is assigned to the vibrational origin of the $\tilde{X}\ ^2\Sigma^+$ state, yielding electron affinities of 3.558 ± 0.015 and 3.552 ± 0.015 eV in C_4H and C_4D, respectively. The electron affinity of C_4H is in reasonable agreement with the value of 3.46 ± 0.07 eV calculated by Natterer and Koch.[84] The signal at higher electron energies than peak $A1$ is most likely due to anion hot bands. We tentatively assign peak a to the $\tilde{X}\ ^2\Sigma^+(\nu_7'=0)\leftarrow\tilde{X}\ ^1\Sigma^+(\nu_7''=1)$ hot band affording a ν_7 frequency in the anion of 210 cm^{-1} and 169 cm^{-1} in $C_4H(D)$, respectively.

Peaks $A1$ and $A2$ are separated by 226 and 210 cm^{-1} in $C_4H(D)$, respectively. They represent the beginning of the ν_7 bending progression in the $^2\Sigma^+$ ground state. Peaks $B1$ and $B2$ belong to the $\tilde{A}\ ^2\Pi$ excited electronic state and are separated by 210 and 185 cm^{-1} in $C_4H(D)$, respectively, indicating the beginning of a second ν_7 bending progression. The appearance of the C_4H^- spectra suggests that peak $B1$ is the origin of the $\tilde{A}$ state, yielding an $\tilde{A}-\tilde{X}$ splitting of 468 cm^{-1}. However, peaks $A2$ and $B1$ are separated by 242 and 258 cm^{-1} in the C_4H^- and C_4D^- spectra, respectively. This is not significantly different from the bending frequencies in both states, so it is possible that the $\tilde{A}$ state origin lies under peak $A2$ or even $A1$. In any case the two electronic states are approximately separated energetically by some integral value of the bending frequency. Endo and co-workers[102] have estimated the $\tilde{A}-\tilde{X}$ splitting in dispersed fluorescence spectra to be 159 and 149 cm^{-1} in $C_4H(D)$, respectively. They did not observe the $\tilde{A}$ state origin directly but make their estimation by extrapolating vibrational progressions in the $\tilde{A}$ state to its origin. Their analysis, if correct, is consistent with the $\tilde{A}$ state origin lying under peak $A2$.

Peaks $C1$ and $C2$ have β parameters indicating that they are from the $\tilde{X}\ ^2\Sigma^+$ state. The spacing between peaks $A1$ and $C1$ is 960 and 895 cm^{-1} in $C_4H(D)$, respectively. This is close to the calculated frequency of 910 cm^{-1} for the ν_4 stretching mode,[30] (lowest frequency C–C stretch) so peaks $C1$ and $C2$ are tentatively assigned to the 4_0^1 and $4_0^1 7_0^1$ transitions. Making assignments in this region is difficult because these peaks are overlapped with pure bending progressions from the $\tilde{X}$ and $\tilde{A}$ states; this is particularly problematic in the C_4D^- spectrum where the individual peaks are less obvious.

Peak D has a β parameter associating it with the $\tilde{A}\ ^2\Pi$ state. It is located 2081 and 2073 cm^{-1} from peak $B1$ in the $C_4H(D)^-$ spectrum, respectively. This is in excellent agreement with the calculated value[30] for the ν_2 frequency (C≡C stretch) of the C_4H $\tilde{A}\ ^2\Pi$ state, 2139 cm^{-1}. The negligible isotopic shift is consistent with the matrix spectroscopy study of Shen *et al.*[82] that showed a very small isotopic shift for the analogous ν_2 mode in the $\tilde{X}\ ^2\Sigma^+$. Peak D is therefore assigned to the 2_0^1 transition to the $\tilde{A}\ ^2\Pi$ state. If peak $A2$ were the $\tilde{A}$ state origin, the same assignment for peak D yields 2323 cm^{-1} for the ν_2 frequency in the $\tilde{A}$ state, which is still close to the calculated value.

The positive β parameter for peak E suggests it is a transition to a vibrational level of the $\tilde{X}\ ^2\Sigma^+$ state. It lies 3065 and 3097 cm^{-1} in $C_4H(D)$, respectively, from peak $A1$. While this is in the range of a C–H stretch, it is considerably lower than the ν_1 frequency of 3307 cm^{-1} observed by Shen *et al.*[82] Moreover, no isotopic shift is observed. Based on the calculated frequencies,[30] the $2_0^1 4_0^1$ combination band should occur at 3193 cm^{-1}, close to the observed energy, and a negligible isotope shift is expected for this transition since both modes are carbon–carbon stretches. However, we do not observe the 2_0^1 transition, which should lie about 2100 cm^{-1} from peak $A1$.[30,82] The next excited electronic state, the $B\ ^2\Pi$ state, lies 3.2 eV above the $\tilde{X}\ ^2\Sigma^+$ state,[78,86,87] so this is not a reasonable assignment for peak E. Assignment to the $2_0^1 4_0^1$ combination band is the most reasonable option but this is clearly problematic.

The peak assignments and energetics for the C_4H^- and C_4D^- spectra are summarized in Tables III and V. Overall, the $C_4H(D)^-$ photoelectron spectra are the most complex of those reported here. The spectra yield an accurate electron affinity and represent the first published observation and characterization of the low-lying $\tilde{A}\ ^2\Pi$ state. They show that this state lies at most only 468 cm^{-1} above the $\tilde{X}\ ^2\Sigma^+$ state.

TABLE III. Peak positions and assignments for the $C_4H(D)^-$ photoelectron spectra.

Peak	Assignment	Position (C_4H)	Splitting from peak $A1$ (cm^{-1})[a]	β[b]	Position (C_4D)	Splitting from peak $A1$ (cm^{-1})[a]	β[b]
a	$\tilde{X}\ 7_1^0$	1.125	−210		1.126	−169	
$A1$	$\tilde{X}\ 0_0^0$	1.099	0	0.29	1.105	0	0.41
$A2$	$\tilde{X}\ 7_0^1$	1.071	226	0.29	1.079	210	0.34
$B1$	$\tilde{A}\ 7_0^n$	1.041	468	0.00	1.047	468	0.22
$B2$	$\tilde{A}\ 7_0^{n+1}$	1.016	669	−0.01	1.024	653	0.10
$C1$	$\tilde{X}\ 4_0^1$	0.980	960	0.62	0.994	895	0.37
$C2$	$\tilde{X}\ 4_0^1 7_0^1$	0.952	1186	0.81	0.959	1178	0.83
D	$\tilde{A}\ 2_0^1$	0.783	2549	−0.37	0.790	2541	−0.17
E	$\tilde{X}\ 2_0^1 4_0^1$	0.715	3065	0.99	0.721	3097	0.77
$F1$					0.404	5654	0.69
$F2$					0.367	5952	0.91
$F3$					0.280	6654	0.52

[a]Error is $\pm 50\ cm^{-1}$.
[b]Average error ± 0.25.

We obtain bending and stretching vibrational frequencies for both electronic states. However, the assignments of several features are not definitive. We hope that the vibronic coupling effects that complicate these spectra will receive more experimental and theoretical attention in the near future.

D. C_6H

The C_6H^- spectra show a different polarization dependence than the C_2H^- and C_4H^- spectra, in that β is *smaller* for peak A, the peak at highest eKE, than for peaks B and C at lower eKE. This suggests that the energy ordering of the two neutral electronic states contributing to this spectrum is reversed, and that the ground state of C_6H is a $^2\Pi$ state, consistent with the earlier microwave spectra[39] and *ab initio* calculations.[83–85,87,91–93] We take peak A to be the vibrational origin of the transition to the $\tilde{X}\ ^2\Pi$ state, yielding an electron affinity of 3.809 ± 0.015 and 3.805 ± 0.015 eV for $C_6H(D)$, respectively. This is in reasonable agreement with values calculated by Feher[93] (3.6 eV) and Natterer[92] (3.69 ± 0.05 eV). No other peaks can be definitively assigned to the $\tilde{X}\ ^2\Pi$ state.

Peaks B and C are assigned to the $\tilde{A}\ ^2\Sigma^+$ first excited state. Peak B is the origin of this state, giving a term value of 0.181 eV. This lies between the values calculated by Sobolewski[87] (0.25 eV) and Woon[85] (0.11 eV). Peak C appears to belong to the $\tilde{A}\ ^2\Sigma^+$ state and we assign it to a vibrational transition with a frequency of 2202 and 2202 cm^{-1} in $C_6H(D)$, respectively. No *ab initio* calculations or experimental values are available for the $\tilde{A}\ ^2\Sigma^+$ state. However, comparison with calculations[89,90] performed on the ground state suggests that a frequency of 2202 cm^{-1} corresponds to the largest C≡C stretching frequency, the ν_2 mode, which corresponds to the triple bond nearest to the H atom. The relative simplicity of these spectra compared to those for C_2H^- and C_4H^- suggests that vibronic coupling plays a significantly smaller role. Peak assignments and energetics for C_6H^- and C_6D^- are summarized in Tables IV and V.

E. C_8H

The polarization dependence of the peaks in the C_8H^- spectra is similar to that in the C_6H^- spectra in that the peaks

TABLE IV. Peak positions and assignments for $C_6H(D)$ and C_8H^- photoelectron spectra. Values in parenthesis are for C_6D.

Molecule	Peak	Assignment	Position	Splitting from peak A (cm^{-1})[a]	β[b]
C_6H	A	$\tilde{X}\ ^2\Pi$	0.848	0	0.22
		origin	(0.852)	(0)	(0.11)
	B	$\tilde{A}\ ^2\Sigma^+$	0.667	1460	0.48
			(0.672)	(1452)	(0.46)
	C	$\tilde{A}\ 2_0^1$	0.394	3662	0.48
			(0.399)	(3654)	(0.45)
C_8H	A	$\tilde{X}\ ^2\Pi$	0.691	0	−0.24
		origin			
	B	$\tilde{X}\ 4_0^1$ or 5_0^1	0.485	1661	−0.29
	C	$\tilde{A}\ ^2\Sigma^+$	0.438	2041	−0.11
	D	$\tilde{A}\ 2_0^1$ or 3_0^1	0.188	4057	−0.04

[a]Error $\pm 50\ cm^{-1}$.
[b]Average error ± 0.25.

TABLE V. Electron affinities for $C_{2n}H(D)$.

Molecule	Present work	Other exp.	*Ab initio*
C_2H	2.956 ± 0.020	2.969 ± 0.006[a]	2.961 ± 0.015[b]
			2.964[c]
			3.09[d]
C_2D	2.954 ± 0.020	2.973 ± 0.006[a]	
C_4H	3.558 ± 0.015		3.46 ± 0.07[e]
C_4D	3.552 ± 0.015		
C_6H	3.809 ± 0.015		3.6[f]
			3.69 ± 0.05[g]
C_6D	3.805 ± 0.015		
C_8H	3.966 ± 0.010		

[a]Reference 68.
[b]Reference 104.
[c]Reference 85.
[d]Reference 105.
[e]Reference 84
[f]Reference 93.
[g]References 84, 92.

at largest eKE have the smallest values of β. We therefore assign peaks *A* and *B* to transitions to the ground $\tilde{X}\ ^2\Pi$ state of C_8H and peaks *C* and *D* to transitions to the low-lying $\tilde{A}\ ^2\Sigma^+$ state. This is consistent with the calculations by Pauzat[83] and Adamowicz[87] that predict a $^2\Pi$ ground state. The position of peak *A* yields an electron affinity of 3.966 ± 0.010 eV. Peak *C* is assigned to the origin of the $\tilde{A}\ ^2\Sigma^+$ state, yielding a term value of 0.253 eV, noticeably lower than the value of 0.52 eV calculated by Adamowicz.[87]

Peaks *B* and *D* correspond to transitions to vibrationally excited levels of the $\tilde{X}\ ^2\Pi$ and $\tilde{A}\ ^2\Sigma^+$ states, respectively. The separation between peaks *A* and *B* is 1661 cm^{-1}. This most likely corresponds to the frequency of modes ν_4 or ν_5, C≡C stretching modes near the carbon terminus. Peak *D* is located 2016 cm^{-1} above peak *C* and corresponds to a high frequency C≡C stretching mode, most likely ν_2 or ν_3. Peak assignments and energetics are summarized in Tables IV and V. No experimental or theoretical values are available for comparison.

V. CONCLUSIONS

The anion photoelectron spectra presented here yield electron affinities for several $C_{2n}H$ radicals and provide information on the vibrational and electronic spectroscopy of these species, including vibrational frequencies and term values for low-lying excited states. All the spectra presented here consist of transitions to two close-lying electronic states of the neutral radical; these transitions can be distinguished and assigned based on the photoelectron angular distributions.

Salient features of the spectra are as follows. The $C_2H(D)^-$ photoelectron spectra were taken at a higher photon energy than in previous work. We observe transitions to several levels of the C_2H $\tilde{X}\ ^2\Sigma^+$ state that lie below the $\tilde{A}\ ^2\Pi$ state, some of which are allowed only by vibronic coupling with the $\tilde{A}\ ^2\Pi$ state. Transitions to levels above the $\tilde{A}\ ^2\Pi$ state origin appear to have considerable $\tilde{A}\ ^2\Pi$ state character even though many of them have previously been assigned to excited vibrational levels of the $\tilde{X}\ ^2\Sigma^+$ state. It thus appears that vibronic coupling between the two states is very strong above the $\tilde{A}\ ^2\Pi$ state origin.

In the $C_4H(D)^-$ photoelectron spectra, transitions to the $\tilde{X}\ ^2\Sigma^+$ and $\tilde{A}\ ^2\Pi$ states of $C_4H(D)$ are even more strongly overlapped than in the $C_2H(D)^-$ spectra; the term value for the $\tilde{A}\ ^2\Pi$ state is no larger than 468 ± 50 cm^{-1}. Extended bending progressions in both states provide evidence of strong vibronic coupling. Such coupling renders a standard Franck-Condon analysis of the spectra virtually useless, and several of the vibrational assignments must be considered as tentative.

The C_6H^- and C_8H^- spectra are simpler than the C_4H^- spectrum, most likely reflecting the larger separation between the ground and first excited states. The photoelectron angular distributions indicate that the ordering of these two electronic states is reversed from the smaller radicals; they have $^2\Pi$ ground states and $^2\Sigma^+$ excited states. To the best of our knowledge, our spectra represent the first experimental observation of the $^2\Sigma^+$ state in both cases. Overall, our spectra confirm trends that have been predicted in previous *ab initio* calculations, namely that the $^2\Pi$ state becomes progressively lower in energy relative to the $^2\Sigma^+$ state as the carbon chain length increases from 2–8.

ACKNOWLEDGMENTS

This work is supported by the National Science Foundation under Grant No. DMR-9521805. The authors would also like to thank Dr. Kennosuke Hoshina and Professor Yasuki Endo for providing us with unpublished results on $C_4H(D)$ and Dr. Gordon R. Burton for early contributions to this project.

[1] W. Weltner and R. Van Zee, Chem. Rev. **89**, 1713 (1989).
[2] S. L. Yang, C. L. Pettiette, J. Conceicao, O. Cheshnovsky, and R. E. Smalley, Chem. Phys. Lett. **139**, 233 (1987).
[3] D. W. Arnold, S. E. Bradforth, T. N. Kitsopoulos, and D. M. Neumark, J. Chem. Phys. **95**, 8753 (1991).
[4] N. Moazzen-Ahmadi, A. R. W. McKellar, and T. Amano, J. Chem. Phys. **91**, 2140 (1989).
[5] N. Moazzen-Ahmadi, A. R. W. McKellar, and T. Amano, Chem. Phys. Lett. **157**, 1 (1989).
[6] P. F. Bernath, K. H. Hinkle, and J. J. Keady, Science **244**, 562 (1989).
[7] J. R. Heath and R. J. Saykally, J. Chem. Phys. **94**, 3271 (1991).
[8] J. R. Heath and R. J. Saykally, in *On Clusters and Clustering, from Atoms to Fractals*, edited by P. J. Reynolds (Elsevier, Amsterdam, 1993), pp. 7–21.
[9] H. J. Hwang, A. Van Orden, K. Tanaka, E. W. Kuo, J. R. Heath, and R. J. Saykally, Mol. Phys. **79**, 769 (1993).
[10] T. F. Giesen, A. Van Orden, H. J. Hwang, R. S. Fellers, R. A. Provencal, and R. J. Saykally, Science **265**, 756 (1994).
[11] C. C. Arnold, Y. X. Zhao, T. N. Kitsopoulos, and D. M. Neumark, J. Chem. Phys. **97**, 6121 (1992).
[12] C. C. Arnold and D. M. Neumark, J. Chem. Phys. **99**, 1442 (1993).
[13] D. Forney, J. Fulara, P. Freivogel, M. Jakobi, D. Lessen, and J. P. Maier, J. Chem. Phys. **103**, 48 (1995).
[14] D. Forney, P. Freivogel, M. Grutter, and J. P. Maier, J. Chem. Phys. **104**, 4954 (1996).
[15] P. Freivogel, J. Fulara, M. Jakobi, D. Forney, and J. P. Maier, J. Chem. Phys. **103**, 54 (1995).
[16] G. von Helden, M. T. Hsu, N. Gotts, and M. T. Bowers, J. Phys. Chem. **97**, 8182 (1992).
[17] K. A. Gingerich, H. C. Finkbeiner, and R. W. Schmude, J. Am. Chem. Soc. **116**, 3884 (1994).
[18] H. Handschuh, G. Gantefor, B. Kessler, P. S. Bechthold, and W. Eberhardt, Phys. Rev. Lett. **74**, 1095 (1995).

[19] K. Raghavachari and J. S. Binkley, J. Chem. Phys. **87**, 2191 (1987).
[20] D. H. Magers, R. J. Harrison, and R. J. Bartlett, J. Chem. Phys. **84**, 3284 (1986).
[21] C. Liang and H. F. Schaefer III, Chem. Phys. Lett. **169**, 150 (1990).
[22] V. Parasuk and J. Almlöf, J. Chem. Phys. **94**, 8172 (1991).
[23] G. Pacchioni and J. Koutecký, J. Chem. Phys. **88**, 1066 (1988).
[24] L. Adamowicz, Chem. Phys. Lett. **182**, 45 (1991).
[25] V. Parasuk and J. Almlöf, J. Chem. Phys. **91**, 1137 (1989).
[26] R. F. Liu and X. F. Zhou, J. Chem. Phys. **99**, 1440 (1993).
[27] S. Schmatz and P. Botschwina, Int. J. Mass Spectrom. Ion Processes **150**, 621 (1995).
[28] S. Schmatz and P. Botschwina, Chem. Phys. Lett. **235**, 5 (1995).
[29] J. M. L. Martin, J. P. Francois, and R. Gijbels, J. Chem. Phys. **93**, 8850 (1990).
[30] J. H. Kiefer, S. S. Sidhu, R. D. Kern, K. Xie, H. Chen, and L. B. Harding, Combust. Sci. Technol. **82**, 101 (1992).
[31] M. Guelin, S. Green, and P. Thaddeus, Astrophys. J. **224**, L27 (1978).
[32] M. Guelin, J. Cernicharo, C. Kahane, J. Gomez-Gonzales, and C. M. Walmsley, Astron. Astrophys. **175**, L5 (1987).
[33] M. Guelin, J. Cernicharo, S. Navarro, D. R. Woodward, C. A. Gottlieb, and P. Thaddeus, Astron. Astrophys. **182**, L37 (1987).
[34] W. M. Irvine, M. Ohishi, and N. Kaifu, Icarus **91**, 2 (1991).
[35] I. A. Crawford, Mon. Not. R. Astron. Soc. **277**, 458 (1995).
[36] J. Cernicharo and M. Guelin, Astron. Astrophys. **309**, L27 (1996).
[37] J. Fulara, D. Lessen, P. Freivogel, and J. P. Maier, Nature (London) **366**, 439 (1993).
[38] C. A. Gottlieb, E. W. Gottlieb, P. Thaddeus, and H. Kawamura, Astrophys. J. **275**, 916 (1983).
[39] J. C. Pearson, C. A. Gottlieb, D. R. Woodward, and P. Thaddeus, Astron. Astrophys. **189**, L13 (1988).
[40] M. C. McCarthy, M. J. Travers, A. Kovacs, C. A. Gottlieb, and P. Thaddeus, Astron. Astrophys. **309**, L31 (1996).
[41] E. L. Cochran, F. J. Adrian, and V. A. Bowers, J. Chem. Phys. **40**, 213 (1965).
[42] W. R. M. Graham, K. I. Dismuke, and W. Weltner, Jr., J. Chem. Phys. **60**, 3817 (1974).
[43] M. Jinguji, C. A. McDowell, and K. Shimokoshi, J. Mol. Struct. **130**, 317 (1985).
[44] R. J. Saykally, L. Veseth, and K. M. Evenson, J. Chem. Phys. **80**, 2247 (1984).
[45] J. M. Brown and K. M. Evenson, J. Mol. Spectrosc. **131**, 161 (1988).
[46] K. V. L. N. Sastry, P. Helminger, A. Charo, E. Herbst, and F. C. de Lucia, Astrophys. J. **251**, L119 (1981).
[47] C. A. Gottlieb, E. W. Gottlieb, and P. Thaddeus, Astrophys. J. **264**, 740 (1983).
[48] M. Bogey, C. Demuynck, and J. L. Destombes, Astron. Astrophys. **144**, L15 (1985).
[49] Y. Endo, H. Kanamori, and E. Hirota, Chem. Phys. Lett. **160**, 280 (1989).
[50] D. E. Milligan, M. E. Jacox, and L. Abouaf-Marguin, J. Chem. Phys. **46**, 4562 (1967).
[51] M. E. Jacox, Chem. Phys. **7**, 424 (1975).
[52] M. E. Jacox and W. B. Olson, J. Chem. Phys. **86**, 3134 (1987).
[53] D. Forney, M. E. Jacox, and W. E. Thompson, J. Mol. Spectrosc. **170**, 178 (1995).
[54] R. A. Shepherd and W. R. M. Graham, J. Chem. Phys. **86**, 2600 (1987).
[55] P. G. Carrick, A. J. Merer, and R. F. Curl, Jr., J. Chem. Phys. **78**, 3652 (1983).
[56] R. F. Curl, P. G. Carrick, and A. J. Merer, J. Chem. Phys. **82**, 3479 (1985).
[57] R. F. Curl, P. G. Carrick, and A. J. Merer, J. Chem. Phys. **83**, 4278 (1985).
[58] W. B. Yan, C. B. Dane, D. Zeitz, J. L. Hall, and R. F. Curl, J. Mol. Spectrosc. **123**, 486 (1987).
[59] W. B. Yan, J. L. Hall, J. W. Stephens, M. L. Richnow, and R. F. Curl, J. Chem. Phys. **86**, 1657 (1987).
[60] J. W. Stephens, Y. Wen-bin, M. L. Richnow, H. Solka, and R. F. Curl, J. Mol. Struct. **190**, 41 (1988).
[61] H. Kanamori, K. Seki, and E. Hirota, J. Chem. Phys. **87**, 73 (1987).
[62] H. Kanamori and E. Hirota, J. Chem. Phys. **88**, 6699 (1988).
[63] H. Kanamori and E. Hirota, J. Chem. Phys. **89**, 3962 (1988).
[64] K. Kawaguchi, T. Amano, and E. Hirota, J. Mol. Spectrosc. **131**, 58 (1988).
[65] M. Vervloet and M. Herman, Chem. Phys. Lett. **144**, 48 (1988).
[66] Y. C. Hsu, J. J. M. Lin, D. Papousek, and J. J. Tsai, J. Chem. Phys. **98**, 6690 (1993).
[67] Y. C. Hsu, Y. J. Shiu, and C. M. Lin, J. Chem. Phys. **103**, 5919 (1995).
[68] K. M. Ervin and W. C. Lineberger, J. Phys. Chem. **95**, 1167 (1991).
[69] M. Peric, R. J. Buenker, and S. D. Peyerimhoff, Mol. Phys. **71**, 673 (1990).
[70] M. Peric, S. D. Peyerimhoff, and R. J. Buenker, Mol. Phys. **71**, 693 (1990).
[71] M. Peric, S. D. Peyerimhoff, and R. J. Buenker, Z. Phys. D **24**, 177 (1992).
[72] J. Zhang, C. W. Riehn, M. Dulligan, and C. Wittig, J. Chem. Phys. **103**, 6815 (1995).
[73] S. H. S. Wilson, C. L. Reed, D. H. Mordaunt, M. N. R. Ashfold, and M. Kawasaki, Bull. Chem. Soc. Jpn. **69**, 71 (1996).
[74] J.-H. Wang, Y.-T. Hsu, and K. Liu, J. Phys. Chem. A **101**, 6593 (1997).
[75] D. H. Mordaunt, M. N. R. Ashfold, R. N. Dixon, P. Loffler, L. Schnieder, and K. H. Welge, J. Chem. Phys. **108**, 519 (1998).
[76] Y. C. Hsu, F. T. Chen, L. C. Chou, and Y. J. Shiu, J. Chem. Phys. **105**, 9153 (1996).
[77] T. R. Fletcher and S. R. Leone, J. Chem. Phys. **90**, 871 (1989).
[78] K. I. Dismuke, W. R. M. Graham, and W. Weltner, Jr., J. Mol. Spectrosc. **57**, 127 (1975).
[79] S. Yamamoto, S. Saito, M. Guelin, J. Cernicharo, H. Suzuki, and M. Ohishi, Astrophys. J. **323**, 149 (1987).
[80] W. Chen, S. E. Novick, M. C. McCarthy, C. A. Gottlieb, and P. Thaddeus, J. Chem. Phys. **103**, 7828 (1995).
[81] M. C. McCarthy, C. A. Gottlieb, P. Thaddeus, M. Horn, and P. Botschwina, J. Chem. Phys. **103**, 7820 (1995).
[82] L. N. Shen, T. J. Doyle, and W. R. M. Graham, J. Chem. Phys. **93**, 1597 (1990).
[83] F. Pauzat, Y. Ellinger, and A. D. McLean, Astrophys. J. **369**, L13 (1991).
[84] J. Natterer and W. Koch, Mol. Phys. **84**, 691 (1995).
[85] D. E. Woon, Chem. Phys. Lett. **244**, 45 (1995).
[86] M. Kolbuszewski, Astrophys. J. **432**, L63 (1994).
[87] A. L. Sobolewski and L. Adamowicz, J. Chem. Phys. **102**, 394 (1995).
[88] K. Hoshina, H. Kohguchi, Y. Ohshima, and Y. Endo, J. Chem. Phys. **108**, 3465 (1998).
[89] T. J. Doyle, L. N. Shen, C. M. L. Rittby, and W. R. M. Graham, J. Chem. Phys. **95**, 6224 (1991).
[90] R. F. Liu, X. F. Zhou, and P. Pulay, J. Chem. Phys. **97**, 1602 (1992).
[91] A. Murakami, K. Kawaguchi, and S. Saito, Publ. Astron. Soc. Jpn. **39**, 189 (1987).
[92] J. Natterer, W. Koch, D. Schroder, N. Goldberg, and H. Schwarz, Chem. Phys. Lett. **229**, 429 (1994).
[93] M. Feher and J. P. Maier, Chem. Phys. Lett. **227**, 371 (1994).
[94] R. B. Metz, A. Weaver, S. E. Bradforth, T. N. Kitsopoulos, and D. M. Neumark, J. Phys. Chem. **94**, 1377 (1990).
[95] C. Xu, G. R. Burton, T. R. Taylor, and D. M. Neumark, J. Chem. Phys. **107**, 3428 (1997).
[96] D. L. Osborn, D. J. Leahy, D. R. Cyr, and D. M. Neumark, J. Chem. Phys. **104**, 5026 (1996).
[97] G. Markovich, R. Giniger, M. Levin, and O. Cheshnovsky, J. Chem. Phys. **95**, 9416 (1991).
[98] B. A. Mamyrin and D. V. Shmikk, Sov. Phys. JETP **49**, 762 (1979).
[99] J. Cooper and R. N. Zare, in *Lectures in Theoretical Physics*, edited by S. Geltman, K. T. Mahanthappa, and W. E. Brittin (Gordon and Breach, New York, 1969), Vol. XI-C, pp. 317–337.
[100] W. B. Yan and T. Amano, J. Chem. Phys. **99**, 4312 (1993).
[101] M. Peric, S. D. Peyerimhoff, and R. J. Buenker, J. Mol. Spectrosc. **148**, 180 (1991).
[102] K. Hoshina and Y. Endo (personal communication).
[103] F. T. Chen, L. C. Chou, and Y. C. Hsu, in *The 22nd International Symposium of Free Radicals* (Doorwerth, The Netherlands, 1993).
[104] J. A. Montgomery and G. A. Petersson, Chem. Phys. Lett. **168**, 75 (1990).
[105] W. I. Sou and W. K. Li, J. Chem. Res.-S, 464 (1995).